

# Light-Induced Reactions of Porous and Single-Crystal Si Surfaces with Carboxylic Acids

Eric J. Lee, Theodore W. Bitner, James S. Ha, Michael J. Shane, and Michael J. Sailor\*

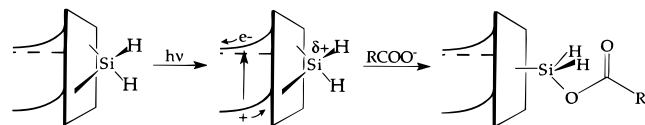
Contribution from the Department of Chemistry and Biochemistry, University of California, San Diego, La Jolla, California 92093-0358

Received March 11, 1996<sup>⊗</sup>

**Abstract:** Light-induced reactions of Si surfaces with carboxylic acids to generate Si ester-modified surfaces are studied. The reaction proceeds by photoelectrochemical oxidation of porous or (100)-oriented single-crystal n-type Si in formic, acetic, or trifluoroacetic acid electrolyte solutions. The reaction products at the porous Si surface are identified by Fourier-transform infrared (FTIR) spectroscopy. Derivatization with esters reduces the photoluminescence intensity of porous Si. X-ray photoelectron spectroscopy (XPS) of derivatized single-crystal Si is used to confirm the compositional and bonding information and to demonstrate that the same chemistry occurs at a single-crystal Si surface. A mechanism is proposed in which illumination of reverse-biased Si removes electron density from the Si surface, rendering Si–Si bonds susceptible to nucleophilic attack by carboxylic acid. The reaction has a marked dependence on light intensity and the Si surface can be photopatterned by illumination through a mask during derivatization. Ester-patterned porous Si reacts with  $\text{CH}_3(\text{CH}_2)_7(\text{CH}_3)_2\text{SiOCH}_3$ , generating an organosilane-patterned Si surface.

Chemical reactions at the surfaces of electronic materials can be very different from the corresponding solution-phase transformations. In particular, the electronic structure of a semiconductor provides a source of electrons or holes that can be used to induce a surface reaction. In this paper, we present a new reaction which modifies the H-terminated surface of porous and single-crystal n-type Si by photoelectrochemical reaction with carboxylic acids, producing a surface-bound silyl ester. The Si surface is activated toward photochemical reaction by applying a positive potential across n-type Si (the reverse-bias condition) in an electrochemical cell. This bends the conduction and valence bands of the Si such that, upon optical excitation, holes migrate to the surface (Scheme 1). Carboxylic acids attack the irradiated, electron-deficient surface, resulting in a surface-bound Si-ester species. Using this simple idea Si surfaces can be photolithographically patterned with esters.

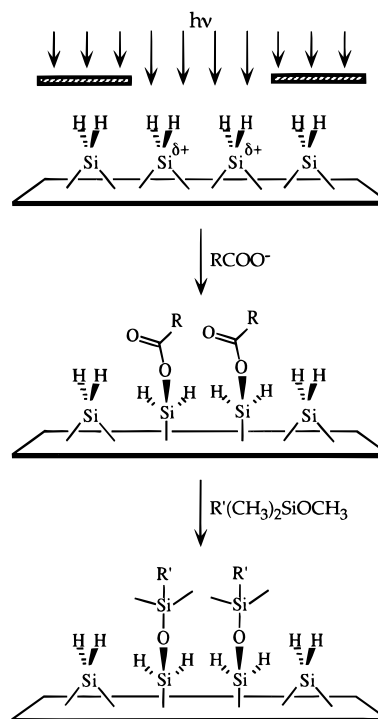
Scheme 1



Esterification significantly changes the reactivity of the Si surface. Organomethoxysilanes react specifically with the esterified region of a photopatterned porous Si sample. This demonstrates a versatile two-step synthetic procedure for patterning Si surfaces with a variety of molecular species (Scheme 2).

Si surface chemistry is very important technologically but does not have an extensive presence in the scientific literature. Much of the chemistry has been done under high vacuum or high temperature reaction conditions.<sup>1</sup> Surface transformations at room temperature and atmospheric pressure generally entail oxidation of the surface in the presence of alkoxy silanes, silyl

Scheme 2



esters, or chlorosilanes.<sup>2,3</sup> Self-assembled monolayers of alkyltrichlorosilanes can be deposited on oxidized Si, probably by self-reaction of the trichlorosilanes in a hygroscopic layer on the surface, followed by bonding to the surface itself.<sup>4</sup> Reactions on non-oxidized Si–H surfaces include radical reactions with alkenes or peroxides.<sup>5,6</sup> Reaction with alcohols to form surface-bound alkoxides can be accomplished electrochemically,<sup>7</sup> or

(2) Maoz, R.; Sagiv, J. *J. Colloid Interface Sci.* **1984**, *100*, 465–496.

(3) Murray, R. W. *Acc. Chem. Res.* **1980**, *13*, 135–141.

(4) Allara, D. L.; Parikh, A. N.; Rondelez, F. *Langmuir* **1995**, *11*, 2357–2360.

(5) Linford, M. R.; Chidsey, C. E. D. *J. Am. Chem. Soc.* **1993**, *115*, 12631–12632.

\* Author to whom correspondence should be addressed.

⊗ Abstract published in *Advance ACS Abstracts*, June 1, 1996.

(1) Waltenburg, H. N.; Yates, J. T. *Chem. Rev.* **1995**, *95*, 1589–1673.

following bromination.<sup>8</sup> These surface reactions generally mirror the chemistry of molecular Si.<sup>9,10</sup> In contrast, the reaction presented here (and in an earlier communication<sup>11</sup>) has no analog in molecular Si chemistry because the semiconductor band structure is an integral part of the reaction mechanism.

Surface chemistry of Si photoelectrodes has been studied in an effort to improve the efficiency and stability of photoelectrochemical solar cells.<sup>12–14</sup> Si photoelectrodes have also been used to polymerize<sup>15,16</sup> and dope<sup>17</sup> polypyrrole films to generate Si/conducting polymer junctions. Chemical modification is also important in large-bandgap semiconductors. For example, derivatization of TiO<sub>2</sub> with a sensitizing dye has been shown to yield an inexpensive high-efficiency solar cell.<sup>18</sup>

Photolithography on Si is a basic technology in the integrated circuit industry.<sup>19</sup> Recent research effort in materials science has led to development of techniques such as scanned probe<sup>20–29</sup> and electron beam<sup>30,31</sup> lithographies which can generate patterns in the submicron to nanometer size regime. Complementing these efforts, materials chemists have focused on manipulating interfacial reactions at the molecular level. This includes generating patterns by physical<sup>32,33</sup> or photochemical<sup>34–40</sup> manip-

ulation of monolayers. For example, Calvert and co-workers have photopatterned Si by derivatizing the surface with phenyltrichlorosilanes and then photochemically cleaving the phenyl–Si bond in the monolayer.<sup>41–44</sup> The work presented in this paper is the first report of chemistry that can pattern Si with a well-defined chemical species by direct photochemical reaction with the Si surface.

## Experimental Section

**Materials.** The Si used was (100) n-type 1 Ω·cm resistivity purchased from International Wafer Service. All chemicals used were purchased from Aldrich, Acros, or the Huls division of United Chemical Technologies.

**Apparatus.** The light source used in the preparation and photochemical derivatization of the silicon samples was a tungsten filament 300-W Kodak ELH bulb with the current controlled by a Variac. Light intensity was monitored with a calibrated photodiode. A Princeton Applied Research Model 363 potentiostat/galvanostat was used in the galvanostatic mode for etching of porous Si samples, and in the potentiostatic mode for the photoderivatization experiments. All electrochemical experiments were performed in a 2-electrode configuration. FTIR spectra were acquired with a Nicolet Model 550 spectrometer in either diffuse reflectance (Spectra-Tech diffuse reflectance attachment) or transmission mode. Diffuse reflectance absorption spectra are reported in Kubelka-Munk units.<sup>45</sup> The FTIR sample compartment was purged with N<sub>2</sub>. X-ray photoelectron spectra were accumulated on a Perkin-Elmer Phi 5100 XPS spectrometer using an Al Kα source.

The electrochemical cell was custom made from Teflon and consists of two pieces, a top with a 1.2 cm diameter cylindrical bore which acts as the solution bath, and a bottom with a 0.2 cm diameter bore and edges cut to fit the FTIR spectrometer transmission-mode sample holder. The Si wafers were cut into squares ca. 2 cm on a side and were secured between the bottom and top of the Teflon cell with two O-rings. Kalrez O-rings were found to withstand the carboxylic acid solutions much better than Viton. The counter electrode was a Pt wire coil. Derivatization with carboxylic acid took place in specially designed glassware which mated to the Teflon electrochemical cell with a No. 116 (3/4 × 15/16 × 3/32 in.) O-ring joint. The derivatization glassware had a window of optical glass opposite the electrochemical cell, a septum-covered opening for introduction of solutions, a 14/20 ground glass joint for securing the coiled Pt wire counter electrode, and a Teflon valve (Kontes). Organosilane reactions were carried out in O-ring sealed Schlenk glassware. Solvent and gas manipulations were performed on a grease-free Schlenk line with Teflon stopcocks using conventional Schlenk and syringe techniques.<sup>46</sup>

**Porous Si Formation.** The Si working electrode was galvanostatically etched in 1:1 49% HF(aq):CH<sub>3</sub>CH<sub>2</sub>OH at 88.5 mA/cm<sup>2</sup> for 2 min while under ~30 mW/cm<sup>2</sup> tungsten lamp illumination. CAUTION: The HF solutions are hazardous and were always handled in an efficient

(6) Linford, M. R.; Fenter, P.; Eisenberger, P. M.; Chidsey, C. E. D. *J. Am. Chem. Soc.* **1995**, *117*, 3145–3155.

(7) Wartjes, M.; Vieillard, C.; Ozanam, F.; Chazalviel, J.-N. *J. Electrochem. Soc.* **1995**, *42*, 4138–4142.

(8) Lee, E. J.; Ha, J. S.; Sailor, M. J. In *Materials Research Society Symposium Proceedings: Microcrystallite and Nanocrystalline Semiconductors*; Collins, R. W., Tsai, C. C., Hirose, M., Koch, F., Brus, L., Eds.; MRS: Pittsburgh, PA, 1995; Vol. 358; pp 387–392.

(9) Pawlenko, S. *Organosilicon Chemistry*; Walter de Gruyter: Berlin, 1986.

(10) Eaborn, C. *Organosilicon Compounds*; Academic Press: New York, 1960.

(11) Lee, E. J.; Ha, J. S.; Sailor, M. J. *J. Am. Chem. Soc.* **1995**, *117*, 8295–8296.

(12) Tufts, B. J.; Kumar, A.; Bansal, A.; Lewis, N. S. *J. Phys. Chem.* **1992**, *96*, 4581–4592.

(13) Bolts, J. M.; Bocarsly, A. B.; Palazzotto, M. C.; Walton, E. G.; Lewis, N. S.; Wrighton, M. S. *J. Am. Chem. Soc.* **1979**, *101*, 1378–1385.

(14) Bard, A. J.; Abruna, H. D.; Chidsey, C. E.; Faulkner, L. R.; Feldberg, S. W.; Itaya, K.; Majda, M.; Melroy, O.; Murray, R. W.; Porter, M. D.; Soriaga, M. P.; White, H. S. *J. Phys. Chem.* **1993**, *97*, 7147–7173.

(15) Inganas, O.; Skotheim, T.; Lundstrom, I. *Phys. Scr.* **1981**, *25*, 863–867.

(16) Yoneyama, H.; Kitayama, M. *Chem. Lett.* **1986**, 657–660.

(17) Inganas, O.; Lundstrom, I. *J. Electrochem. Sci.* **1984**, *131*, 1129–1132.

(18) O'Regan, B.; Gratzel, M. *Nature* **1991**, *353*, 737–740.

(19) Moreau, W. M. *Semiconductor Lithography; Principles, Practices, and Materials*; Plenum Press: New York, 1988.

(20) Snow, E. S.; Campbell, P. M. *Science* **1995**, *270*, 1639–1641.

(21) Sohn, L. L.; Willett, R. L. *Appl. Phys. Lett.* **1995**, *67*, 1552–1554.

(22) Muller, W. T.; Klein, D. L.; Lee, T.; Clarke, J.; McEuen, P. L.; Schultz, P. G. *Science* **1995**, *268*, 272–273.

(23) *The Technology of Proximal Probe Lithography*; Marrian, C. R. K., Ed.; SPIE: Bellingham, WA, 1993.

(24) Quate, C. F. In *Highlights in Condensed Matter Physics and Future Prospects*; Esaki, L., Ed.; Plenum: New York, 1991.

(25) Schoer, J. K.; Ross, C. B.; Crooks, R. M.; Corbitt, T. S.; Hampden-Smith, M. J. *Langmuir* **1994**, *10*, 615–618.

(26) Perkins, F. K.; Dobisz, E. A.; Brandow, S. L.; Koloski, T. S.; Calvert, J. M.; Rhee, K. W.; Kosakowski, J. E.; Marrian, C. R. K. *J. Vac. Sci. Technol. B* **1994**, *12*, 3725–3730.

(27) Dagata, J. A.; Schneir, J.; Haray, H. H.; Evans, C. J.; Postek, M. T.; Bennett, J. *Appl. Phys. Lett.* **1990**, *56*, 2001–2003.

(28) Kobayashi, A.; Grey, F.; Williams, R. S.; Aono, M. *Science* **1993**, *259*, 1724–1726.

(29) Perkins, F. K.; Dobisz, E. A.; Brandow, S. L.; Calvert, J. M.; Kosakowski, J. E.; Marrian, C. R. K. *Appl. Phys. Lett.* **1996**, *68*, 550–552.

(30) Marrian, C. R. K.; Perkins, F. K.; Brandow, S. L.; Koloski, T. S.; Dobisz, E. A.; Calvert, J. M. *Appl. Phys. Lett.* **1994**, *64*, 390–392.

(31) Lercel, M. J.; Redinbo, G. F.; Rooks, M.; Tiberio, R. C.; Craighead, H. G.; Sheen, C. W.; Allara, D. L. *Microelectron. Eng.* **1995**, *27*, 43–46.

(32) Kumar, A.; Biebuyck, H. A.; Whitesides, G. M. *Langmuir* **1994**, *10*, 1498–1511.

(33) Jackman, R. J.; Wilbur, J. L.; Whitesides, G. M. *Science* **1995**, *269*, 664–666.

(34) Bhatia, S. K.; Hickman, J. J.; Ligler, F. S. *J. Am. Chem. Soc.* **1992**, *114*, 4432–4433.

(35) Huang, J.; Dahlgren, D. A.; Hemminger, J. C. *Langmuir* **1994**, *10*, 626–628.

(36) Wollman, E. W.; Kang, D.; Frisbie, C. D.; Lorkovic, I. M.; Wrighton, M. S. *J. Am. Chem. Soc.* **1994**, *116*, 4395–4404.

(37) Kang, D.; Wrighton, M. S. *Langmuir* **1991**, *7*, 2169–2174.

(38) Rozsnyai, L. F.; Benson, D. R.; Fodor, S. P. A.; Schultz, P. G. *Angew. Chem., Int. Ed. Engl.* **1992**, *31*, 759–761.

(39) Rozsnyai, L. F.; Wrighton, M. S. *Langmuir* **1995**, *11*, 3913–3920.

(40) Wolf, M. O.; Fox, M. A. *J. Am. Chem. Soc.* **1995**, *117*, 1845–1846.

(41) Dulcey, C. S.; Georger, J. H., Jr.; Krauthamer, V.; Stenger, D. A.; Fare, T. L.; Calvert, J. M. *Science* **1991**, *252*, 551–554.

(42) Calvert, J. M. *J. Vac. Sci. Technol. B* **1993**, *11*, 2155–2163.

(43) Dressick, W. J.; Calvert, J. M. *Jpn. J. Appl. Phys.* **1993**, *32*, 5829–5839.

(44) Dressick, W. J.; Dulcey, C. S.; Georger, J. H., Jr.; Calvert, J. M. *Chem. Mater.* **1993**, *5*, 148–150.

(45) Ferraro, J. R.; Rein, A. J. In *Fourier Transform Infrared Spectroscopy—Applications to Chemical Systems*; Ferraro, J. R., Basile, L. J., Eds.; Academic Press: New York, 1985; Vol. 4, pp 243–282.

(46) Shriver, D. F.; Drezdson, M. A. *The Manipulation of Air-Sensitive Compounds*, 2nd ed.; John Wiley and Sons, Inc: New York, 1986.

fume hood. The resulting porous layer was washed thoroughly with  $\text{CH}_2\text{Cl}_2$  (in air) and dried under a  $\text{N}_2$  stream.

The etch conditions were chosen to produce a thin, photoluminescent layer with large-diameter pores.<sup>47</sup> An etch time of less than 2 min resulted in porous layers that were not photoluminescent. A current density of  $88.5 \text{ mA/cm}^2$ , near the electrochemical polishing regime, was found to produce large-diameter pores. The etch conditions were chosen to make a layer that was photoluminescent yet thin enough to retain sufficient electrical conductivity through the layer.

**Ester Derivatization.** An electrolyte solution of  $\text{HCOOH}/1 \text{ M HCOONa}$  or  $\text{CF}_3\text{COOH}/1 \text{ M CF}_3\text{COONa}$  was degassed by repeated freeze–pump–thaw cycles and then transferred by cannula into the derivatization glassware described above. Derivatization proceeded at a constant applied bias of either 0.3 or 0.5 V versus the Pt counter electrode for formic acid or 1 V for trifluoroacetic acid reactions, and at a light intensity of typically  $20 \text{ mW/cm}^2$ . The reaction proceeded for 10–20 min, after which the Si was removed from the cell, washed successively with  $\text{CH}_3\text{CN}$  and  $\text{CH}_2\text{Cl}_2$ , and dried under a  $\text{N}_2$  stream. It was found that if the samples were not thoroughly rinsed, formic acid remained adsorbed to the surface, as observed by an apparent shift in the ester  $\nu(\text{C}=\text{O})$  band in the infrared spectrum (from  $1710 \text{ cm}^{-1}$  to between  $1710$  and  $1720 \text{ cm}^{-1}$ , depending on the amount of free formic acid present). The esterification reactions were followed as a function of time by analyzing a series of identically-etched porous Si samples that were reacted for different lengths of time.

Single-crystal (100)-oriented Si was generally derivatized with  $\text{CH}_3\text{-COOH}/0.3 \text{ M CH}_3\text{COONa}$ . The native Si oxide was removed prior to derivatization by immersion in 1% aqueous HF for 5 min and rinsing with  $\text{H}_2\text{O}$  for 5 min.<sup>48</sup> This removed surface oxide and fluoride to below the detection limit of our X-ray photoelectron spectrometer. Sodium acetate was stored and weighed under  $\text{N}_2$  atmosphere to avoid incorporation of atmospheric  $\text{H}_2\text{O}$ . Acetic acid (99.99%, Aldrich) was added to the  $\text{CH}_3\text{COONa}$  under  $\text{N}_2$  purge and the solution freeze–pump–thaw degassed three times before addition to the electrochemical cell. Photoelectrolysis proceeded for 2 min at an applied bias of +1 V vs the Pt counter electrode. Samples were exposed to 10–20  $\text{mW/cm}^2$  tungsten lamp illumination for the duration of photoelectrolysis.

The concentration of formate ester on porous Si as a function of photoderivatization light intensity was measured by irradiating different identically prepared samples for 5 min at 0.5 V bias under various light intensities. Light intensity was controlled by changing the current into the tungsten light source by means of a Variac. Light intensity was monitored by an Ealing Electro-Optics Model 27-6527 calibrated photodiode.

Photopatterned samples were generated by imaging a square mask placed in front of the light source through a Vivitar 70–180 mm zoom camera lens onto the Si surface.

The reaction with organosilane was conducted with a 1% solution of  $\text{CH}_3(\text{CH}_2)_7(\text{CH}_3)_2\text{SiOCH}_3$  in distilled toluene, freeze–pump–thaw degassed three times. The organosilane solution was transferred by cannula into an evacuated container holding the Si wafer and allowed to react at room temperature for 3 h. The derivatized surface was then washed with toluene and  $\text{CH}_2\text{Cl}_2$  and dried under a  $\text{N}_2$  stream.

## Results and Discussion

**FTIR Spectroscopy of Modified Porous Si Surfaces.** Si is transparent in the fingerprint infrared wavelength region (unless it is highly doped) and transmission FTIR spectra can be conveniently taken through the Si wafer. The Si substrates were etched in HF to produce a high surface area porous layer,<sup>49,50</sup> which aids in the spectroscopic identification of surface species. The surface of as-etched porous Si is hydride-terminated. The FTIR spectrum (Figure 1, initial spectrum) consists solely of  $\nu(\text{Si}-\text{H}_x)$  stretching modes at  $2089 \text{ cm}^{-1}$  for  $\nu(\text{Si}-\text{H})$ ,  $2116 \text{ cm}^{-1}$  for  $\nu(\text{Si}-\text{H}_2)$ , and  $2139 \text{ cm}^{-1}$  for

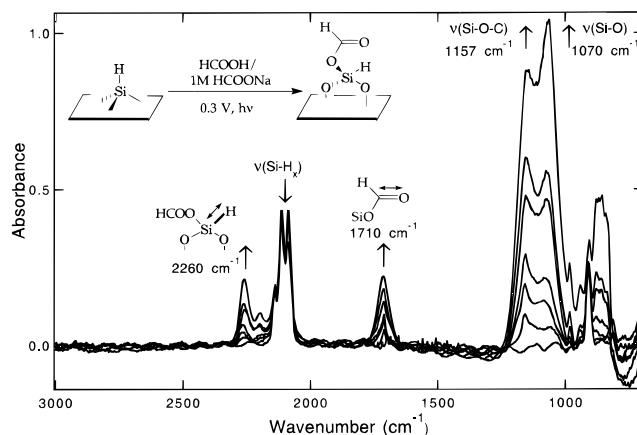


**Figure 1.** Series of FTIR spectra of porous Si surfaces taken following photoelectrochemical reaction with  $\text{HCOOH}/1 \text{ M HCOONa}$  for 0, 1, 3, 5, 10, 18, and 30 min.  $\nu(\text{Si}-\text{H})$  absorptions at  $2089 \text{ cm}^{-1}$  decrease while the  $\nu(\text{OSi}-\text{H})$  absorptions at  $2260 \text{ cm}^{-1}$  and the  $\nu(\text{C}=\text{O})$  of the silyl ester at  $1710 \text{ cm}^{-1}$  increase over time. A  $\nu(\text{Si}-\text{O}-\text{C})$  vibration at  $1157 \text{ cm}^{-1}$  and a  $\nu(\text{Si}-\text{O})$  stretch at  $1070 \text{ cm}^{-1}$  also appear and grow.

$\nu(\text{Si}-\text{H}_3)$ . A  $\delta(\text{Si}-\text{H}_2)$  scissor mode absorption is present at  $908 \text{ cm}^{-1}$ .<sup>51,52</sup>

The Si–H surface is derivatized with formic ester by photoelectrolysis in  $\text{HCOOH}/1 \text{ M HCOONa}$ . Figure 1 shows the evolution of the FTIR spectrum of the porous Si surface during the course of the reaction. An absorption grows in around  $1070 \text{ cm}^{-1}$ , assigned to a  $\nu(\text{Si}-\text{O})$  stretching mode.<sup>53</sup> A second absorption at  $1157 \text{ cm}^{-1}$  also appears, and is assigned to an asymmetric  $\nu(\text{Si}-\text{O}-\text{C})$  stretch.<sup>7,54,55</sup> The appearance and growth of an absorption at  $1710 \text{ cm}^{-1}$  is also observed and is assigned to the stretching mode of the Si ester carbonyl. Shifts in the carbonyl stretching frequency are useful fingerprints for changes in its chemical environment. The  $\nu(\text{C}=\text{O})$  stretch of the formic acid starting material is at  $1720 \text{ cm}^{-1}$ , while the stretching frequency expected for silyl formic esters is around  $1710 \text{ cm}^{-1}$ .<sup>54</sup>

In the hydride stretching region of the spectra, the intensity of the  $\nu(\text{Si}-\text{H})$  and  $\nu(\text{Si}-\text{H}_2)$  absorptions decreases over the course of the reaction, with monohydride experiencing the greatest loss. Concomitantly, an absorption above  $2260 \text{ cm}^{-1}$  grows in. This higher frequency absorption is assigned to a  $\nu(\text{Si}-\text{H})$  stretch from a Si atom that is back-bonded to an O atom of the ester ( $\nu(\text{OSi}-\text{H})$ ). The  $\nu(\text{OSi}-\text{H})$  stretch from a simple oxide surface (prepared by photoelectrolysis in  $\text{H}_2\text{O}/0.1 \text{ M NaCl}$ ) occurs at  $2250 \text{ cm}^{-1}$ .<sup>56–58</sup> The ester-back-bonded absorption is shifted to higher energy because the formate ester species has a greater inductive effect than a simple oxide.<sup>54</sup>

The presence of the  $\nu(\text{Si}-\text{O}-\text{C})$  absorption, the presence and position of the  $\nu(\text{C}=\text{O})$  absorption, and the position of the  $\nu(\text{OSi}-\text{H})$  absorption indicate that a molecular ester species is bonded to the surface. Binding in a bidentate carboxylate mode as observed on some metal oxides is ruled out because such a species is expected to have three absorptions between  $1600$  and  $1400 \text{ cm}^{-1}$ ,<sup>59,60</sup> which were not observed.

(51) Chabal, Y. J. *Physica B* **1991**, 170, 447–456.

(52) Chabal, Y. J. *J. Mol. Struct.* **1993**, 292, 65–80.

(53) Gupta, P.; Dillon, A. C.; Bracker, A. S.; George, S. M. *Surf. Sci.* **1991**, 245, 360–372.

(54) Anderson, D. R. In *Analysis of Silicones*; Smith, A. L., Ed.; Wiley and Sons: New York, 1974; pp 247–286.

(55) Glass, J. A.; Wovchko, E. A.; Yates, J. T. *Surf. Sci.* **1995**, 338, 125–137.

(56) Kato, Y.; Ito, T.; Hiraki, A. *Appl. Surf. Sci.* **1989**, 41/42, 614–618.

(57) O'Keeffe, P.; Aoyagi, Y.; Komura, S.; Kato, T.; Morikawa, T. *Appl. Phys. Lett.* **1995**, 66, 836–838.

(58) Yamada, M.; Kondo, K. *Jpn. J. Appl. Phys.* **1992**, 31, L993–L996.

(47) Smith, R. L.; Collins, S. D. *J. Appl. Phys.* **1992**, 71, R1–R18.

(48) Bjorkman, C. H.; Alay, J. L.; Nishimura, H.; Fukuda, M.; Yamazaki, T.; Hirose, M. *Appl. Phys. Lett.* **1995**, 67, 2049–2051.

(49) Canham, L. T. *Appl. Phys. Lett.* **1990**, 57, 1046–1048.

(50) Lehmann, V.; Gosele, U. *Appl. Phys. Lett.* **1991**, 58, 856–858.

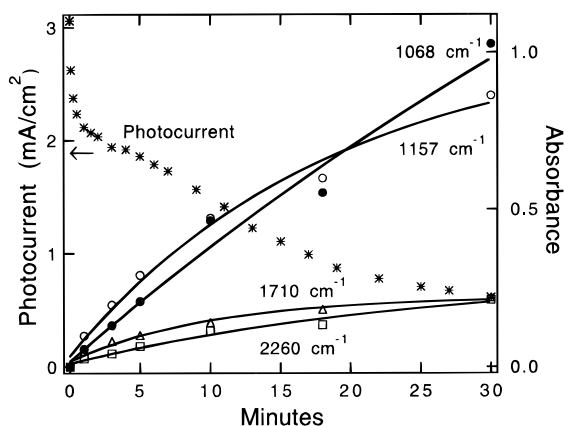


**Figure 2.** Plot of the absorbance of the  $\nu(\text{OSi-H})$  (□, 2260  $\text{cm}^{-1}$ ),  $\nu(\text{C=O})$  (Δ, 1710  $\text{cm}^{-1}$ ),  $\nu(\text{Si-O-C})$  (○, 1157  $\text{cm}^{-1}$ ), and  $\nu(\text{Si-O})$  (●, 1068  $\text{cm}^{-1}$ ) vibrations as a function of the photoesterification reaction time. The absorptions associated with the surface-bound ester ( $\nu(\text{OSi-H})$ ,  $\nu(\text{C=O})$ ,  $\nu(\text{Si-O-C})$ ) all grow in at roughly the same rate. The  $\nu(\text{Si-O})$  absorption, assigned to both surface oxide and oxide associated with the ester, increases faster at longer times relative to the other absorptions, indicating that some conversion of the formate species to surface oxide occurs during the formate derivatization reaction. The photocurrent measured during the course of the 30-min reaction (\*) is plotted on the left axis.

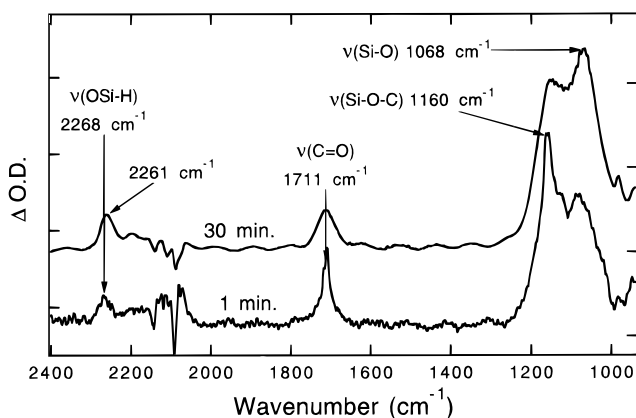


**Figure 3.** Difference spectra after 1 (lower) or 30 min (upper) of photoelectrolysis in  $\text{HCOOH}/1 \text{ M HCOONa}$ . The spectrum after 1 min is that of the predominantly ester-modified surface, while after 30 min the surface has a significant amount of the simple oxide present as well.

The  $\nu(\text{OSi-H})$ ,  $\nu(\text{C=O})$ ,  $\nu(\text{Si-O-C})$ , and  $\nu(\text{Si-O})$  absorptions grow in at approximately the same rate (Figure 2), with  $\nu(\text{Si-O})$  growing in faster than  $\nu(\text{Si-O-C})$  at longer times. This indicates some conversion of the molecular ester to surface oxide over time, which may occur by reaction with trace moisture or by production of an ester anhydride and  $\text{Si-O-Si}$  from adjacent ester sites.<sup>61</sup> The partial conversion of Si ester to simple oxide can be seen in difference IR spectra taken after 1 and 30 min of reaction. In Figure 3, the difference spectrum taken 1 min into the reaction shows growth of a large absorption at 1160  $\text{cm}^{-1}$  assigned to  $\nu(\text{Si-O-C})$  stretches and a smaller absorption around 1068  $\text{cm}^{-1}$  assigned to a  $\nu(\text{Si-O})$  stretching mode. The  $\nu(\text{OSi-H})$  band appears at 2268  $\text{cm}^{-1}$ . The spectral data after 1 min are assigned to the ester-modified surface in the absence of significant surface oxide. The difference spectrum after 30 min of reaction shows the  $\nu(\text{Si-O})$ ,  $\nu(\text{Si-O-C})$ , and  $\nu(\text{C=O})$  absorptions at the same frequencies as after 1 min. However, the  $\nu(\text{Si-O})$  absorption peak at 1068  $\text{cm}^{-1}$  is now more intense than the  $\nu(\text{Si-O-C})$  absorption. The  $\nu(\text{OSi-H})$  stretching frequency has shifted to 2261  $\text{cm}^{-1}$  after 30 min. The shift in frequency of the  $\nu(\text{OSi-H})$  absorption over the course of the reaction is attributed to partial conversion of Si ester to the simple  $\text{Si-O-Si}$  oxide. Assuming the value of 2268  $\text{cm}^{-1}$  to be the  $\nu(\text{OSi-H})$  stretching frequency for the ester-bonded species and 2250  $\text{cm}^{-1}$  to be that of the simple oxide, the  $\nu(\text{OSi-H})$  band observed at 2261  $\text{cm}^{-1}$  after 30 min indicates that the surface is comprised of approximately 55% ester and 45% simple oxide. Soaking the ester-modified Si in acidic water hydrolyzes off the ester species within 15 min, generating a  $\nu(\text{OSi-H})$  signal in the infrared spectrum at 2251  $\text{cm}^{-1}$ .

During the derivatization reaction, illumination of the porous Si electrochemical cell produces a photocurrent. The current presumably arises primarily from a photo-Kolbe reaction in the carboxylate electrolyte, oxidizing  $\text{RCOO}^-$  to  $\text{R}^\bullet$  and  $\text{CO}_2$ .<sup>62,63</sup> The photocurrent is initially several  $\text{mA}/\text{cm}^2$  but decreases over time as the surface becomes oxidized (Figure 2). After 30 min of reaction, the photocurrent is one-fourth its original value. There is no simple correlation between the photocurrent and the rate of surface modification. Both the photocurrent and the surface modification rate can be increased by increasing the applied bias. The electrochemistry generates the same infrared spectroscopic features up to +10 V. At applied bias voltages greater than +10 V a surface species with a sharp absorption band at 2341  $\text{cm}^{-1}$  appeared. The nature of this species has not yet been determined.

Control samples were prepared by an identical derivatization procedure except that the Si electrode was not illuminated during electrolysis. Without illumination there was only a small, steady dark current of  $<0.05 \text{ mA}/\text{cm}^2$  at the +0.3 V applied potential. Infrared analysis of the surfaces after the reaction showed no evidence of ester formation. As a second control experiment, the Si was illuminated at open circuit. Again, no ester or oxide was observed in the subsequent FTIR spectrum. Another sample was prepared which was illuminated at short circuit. The photocurrent alone was sufficient to esterify the surface, though at a much slower rate than samples with an applied bias.

Other types of Si ester surface species may be generated by reaction with the appropriate carboxylic acid. Photoelectrochemical derivatization in  $\text{CF}_3\text{COOH}/1 \text{ M CF}_3\text{COONa}$  produces a silyl trifluoroacetic ester-terminated surface. Reaction with  $\text{CF}_3\text{COOH}/1 \text{ M CF}_3\text{COONa}$  is slower than with  $\text{HCOOH}/1 \text{ M HCOONa}$ , due to either a difference in the rate of nucleophilic attack or to the lower conductivity of the trifluoroacetic acid electrolyte solution. The slower rate was compensated by increasing the applied voltage to +1 V. Figure 4 shows the difference spectrum before and after reaction for 12 min under 10–20  $\text{mW}/\text{cm}^2$  white light.  $\nu(\text{Si-H})$  and  $\nu(\text{Si-H}_2)$  absorptions are found to disappear at the same rate. A  $\nu(\text{OSi-H})$  absorption appears at 2262  $\text{cm}^{-1}$ . Absorptions assigned to the  $\text{CF}_3$  group of surface-bound  $\text{CF}_3\text{C(O)O-}$  are observed at 1377  $\text{cm}^{-1}$ . The  $\nu(\text{C=O})$  carbonyl absorption from the trifluoroacetic ester is at 1772  $\text{cm}^{-1}$ . By comparison, the carbonyl of free  $\text{CF}_3\text{COOH}$  absorbs at 1785  $\text{cm}^{-1}$ . The spectrum taken of a model compound for this surface,  $(\text{CH}_3)_3\text{SiOC(O)CF}_3$ , has a carbonyl stretching absorption at 1772  $\text{cm}^{-1}$ , identical to that of the product surface. In addition, the  $\nu(\text{Si-O-C})$  stretch for the model compound appears at 1168  $\text{cm}^{-1}$ , while the same

(59) Crowell, J. E.; Chen, J. G.; Yates, J. T., Jr. *J. Chem. Phys.* **1986**, *85*, 3111–3122.

(60) Allara, D. L.; Nuzzo, R. G. *Langmuir* **1985**, *1*, 45–52.

(61) Yurev, Y. K.; Belyakova, Z. V. *Russian Chem. Rev.* **1960**, *29*, 383–394.

(62) Schafer, H.-J. In *Electrochemistry IV*; Steckhan, E., Ed.; Springer-Verlag: Berlin, 1990; Vol. 152, pp 91–144.

(63) Bard, A. J. *Science* **1980**, *207*, 139–144.

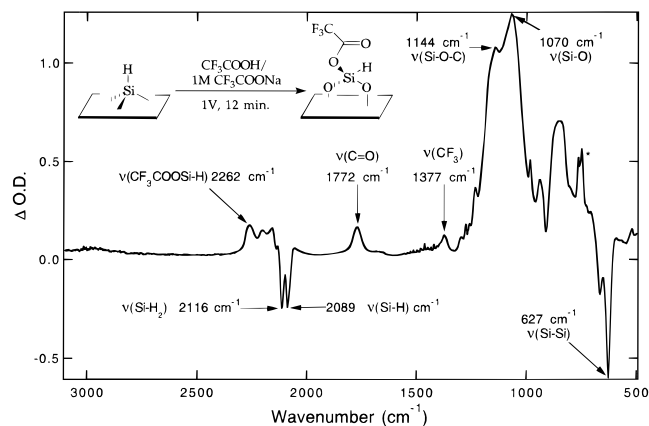


**Figure 4.** Infrared spectrum representing the difference before and after reaction of porous Si with  $\text{CF}_3\text{COOH} / 1 \text{ M } \text{CF}_3\text{COONa}$ . The intensities of the bands assigned to  $\nu(\text{Si-H})$  and  $\nu(\text{Si-H}_2)$  decrease, while a band assigned to  $\nu(\text{OSi-H})$  at  $2262 \text{ cm}^{-1}$  appears. In addition, vibrational bands assigned to the surface-bound trifluoroacetate group appear upon reaction. The band marked with an asterisk is assigned to residual  $\text{CH}_2\text{Cl}_2$  from the sample rinse.

stretch for the surface-bound species appears at  $1144 \text{ cm}^{-1}$ . The IR absorption at  $627 \text{ cm}^{-1}$  is believed to arise from Si-Si surface bonds.<sup>64</sup> This absorption is found to decrease after reaction.

Other oxygen-containing nucleophiles such as water, alcohols, and sulfuric acids were studied to identify reagents that will attack the positively charged illuminated surface but not the non-illuminated surface. Water readily formed the  $\text{SiO}_2$  simple oxide when Si was electrolyzed in  $\text{H}_2\text{O}/0.1 \text{ M } \text{NaCl}$  in either the light or the dark.<sup>65</sup> Photoelectrolysis in alcoholic electrolyte solutions dissolves porous Si.<sup>7,65</sup> Sulfuric acid was not very reactive with either illuminated or non-illuminated reverse-biased porous Si. Of the reagents examined, carboxylic acids alone were found to selectively react with the positively charged, illuminated surface.

**X-ray Photoelectron Spectroscopy of Modified Single-Crystal Si Surfaces.** X-ray Photoelectron Spectroscopy (XPS) was used to confirm the elemental and bonding information of FTIR spectroscopy on the porous Si surfaces, and to demonstrate that the same chemistry occurs at a single-crystal Si surface (Figure 5).<sup>12,66-69</sup> The (100) face of single-crystal Si was derivatized in  $\text{CH}_3\text{COOH}/0.5 \text{ M } \text{CH}_3\text{COONa}$  at +1 V applied bias under illumination for 2 min. A photocurrent density of  $0.100 \text{ mA/cm}^2$  developed upon application of bias and decayed to zero by 1.5 min. The resulting surfaces were oxidized, as indicated by a strong signal at a binding energy of 103.1 eV (assigned to  $\text{SiO}_x$ ) in the Si region of the XPS spectrum. In the C binding energy region of the XPS spectrum, a signal observed at 289.6 eV is assigned to the carbonyl C of the acetic ester.<sup>69,70</sup> The signal arising from the C atom of the methyl group is obscured by the adventitious hydrocarbon peak at 285 eV. A control sample was electrolyzed in the same manner

(64) Theiss, W.; Grosse, P.; Munder, H.; Luth, H.; Herino, R.; Ligeon, M. *Appl. Surf. Sci.* **1993**, *63*, 240-244.

(65) Lee, E. J.; Bitner, T. W.; Hall, A. P.; Sailor, M. J. *J. Vac. Sci. Technol. A* In press.

(66) Kallury, K. M. R.; Krull, U. J.; Thompson, M. *Anal. Chem.* **1988**, *60*, 169-172.

(67) Lee, S.; Makan, S.; Holl, M. M. B.; McFeely, F. R. *J. Am. Chem. Soc.* **1994**, *116*, 11819-11826.

(68) Raider, S. I.; Flitsch, R. *IBM J. Res. Develop.* **1978**, *22*, 294-303.

(69) Wagner, C. D.; Riggs, W. M.; Davis, L. E.; Moulder, J. F.; Muilenberg, G. E. *Handbook of X-Ray Photoelectron Spectroscopy*; Perkin-Elmer Corporation: Eden Prairie, MN, 1978.

(70) Gelius, U.; Heden, P. F.; Hedman, J.; Lindberg, B. J.; Manne, R.; Nordberg, R.; Nordling, C.; Siegbahn, K. *Phys. Scr.* **1970**, *2*, 70-80.

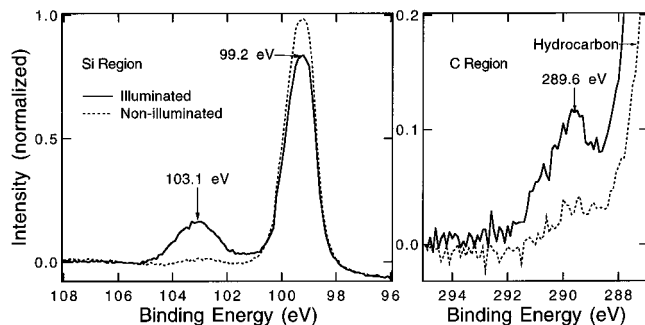


**Figure 5.** XPS data of single-crystal Si following electrolysis in  $\text{CH}_3\text{COOH}/0.5 \text{ M } \text{CH}_3\text{COONa}$  with and without illumination. The sample prepared under illumination is oxidized, as indicated by the signal at 103.1 eV in the Si binding energy region. In the C binding energy region, a carbonyl C signal is apparent at 289.6 eV. The non-illuminated sample displays no indication of significant oxide or carbonyl species. Signal intensities are normalized against total Si (Si and  $\text{SiO}_x$ ) intensity.

but without illumination. This sample passed no detectable current upon application of bias. The XPS data indicate that no significant oxidation of the Si or incorporation of surface carbonyl occurred. Electrolysis of Si in neat formic acid was also found to oxidize Si in the light, but not in the dark.

Trifluoroacetic acid electrolyte solutions modify the single-crystal surfaces as well, although without as much discrimination between illuminated and non-illuminated samples. XPS spectra of samples prepared under illumination show a peak around 103 eV assigned to Si oxide, C signals from  $\text{CF}_3$  at 290.5 eV, carbonyl C at 289.5 eV, and F signals from  $\text{CF}_3$  at 687 eV and a smaller signal at 686 eV from Si-F.<sup>69</sup> Electrolysis of Si in trifluoroacetate solution in the dark generates a surface with an XPS spectrum similar to that of the illuminated sample, except that the peaks assigned to trifluoroacetic ester are  $1/3$  to  $1/4$  as intense. Trifluoroacetate solutions also reacted slowly with single-crystal Si simply upon contact.

Reactions on single-crystal Si are much more sensitive to trace water contamination than are those on porous Si. Small amounts of moisture in the acetic acid electrolyte solutions of the control experiments in the dark result in the observation of a small dark current and slight oxidation of the Si. Porous Si samples are more tolerant of trace moisture in the derivatizing solution probably because the subsequent dark current is largely suppressed by the resistive porous layer. Another difference between porous and single crystal Si is that the porous Si exposes several different crystal faces to the derivatizing solution. The relative reactivities of the different crystal faces have not yet been studied.

**Reaction Mechanism.** Examination of the IR spectra before and after derivatization indicates that the reaction proceeds by breaking Si-Si bonds rather than Si-H bonds. In the Si-H<sub>x</sub> stretching region, difference spectra before and after reaction show no loss of net absorbance from Si-H and OSi-H. In fact, the total area under Si-H and OSi-H absorption bands increases as the OSi-H band grows in, indicating that hydride coverage is increasing at the same time the surface is being esterified. Photoelectrolysis in DCOOD (with 10%  $\text{D}_2\text{O}/1 \text{ M } \text{DCOONa}$ ) produced  $\nu(\text{Si-D})$  and  $\nu(\text{OSi-D})$  bands at 1530 and  $1630 \text{ cm}^{-1}$ , respectively, the latter as a shoulder on the carbonyl stretch at  $1682 \text{ cm}^{-1}$ , Figure 6 (the main  $\nu(\text{C=O})$  stretch for free DCOOD occurs at  $1692 \text{ cm}^{-1}$ ). Neither Si-D nor OSi-D was observed upon photoelectrolysis with HCOOD/HCOONa solutions, indicating that the extra surface hydrides are formed by abstraction of  $\text{H}^\bullet$  from the carbon atom of formate and not from the acidic proton. Reaction with  $\text{CF}_3\text{COOH}$  generates

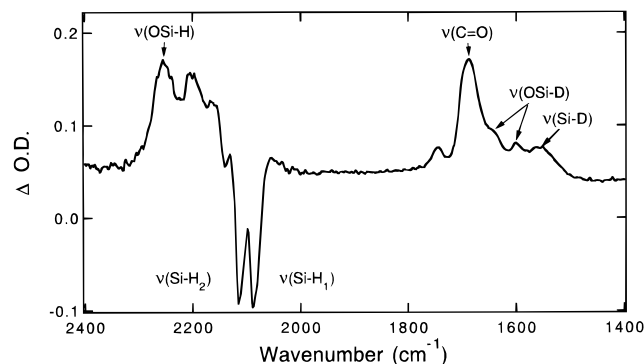


**Figure 6.** FTIR spectra of a porous Si sample derivatized with DCOOD/1 M DCOONa. Absorptions due to  $\nu(\text{Si-H}_i)$  decrease, and those due to  $\nu(\text{Si-D}_i)$ ,  $\nu(\text{OSi-D})$ , and  $\nu(\text{OSi-H})$  form, demonstrating that the Si surface picks up D from the solution during the reaction.

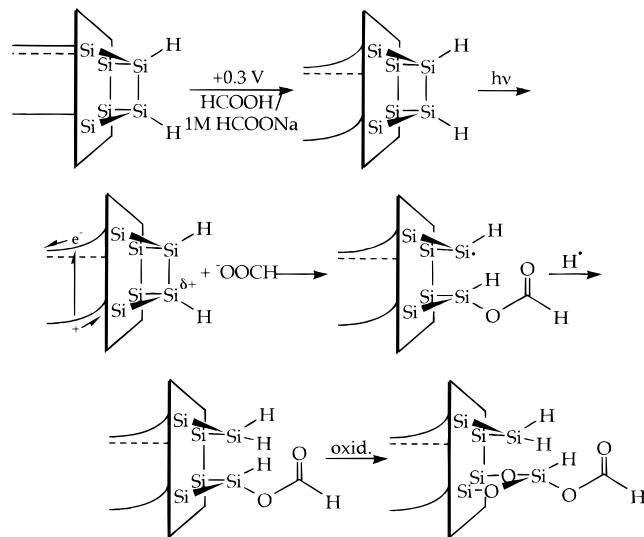


**Figure 7.** Proposed photoesterification reaction mechanism. The conduction and valence bands and Fermi level for the semiconductor substrate are depicted to the left of each surface. Immersion in the electrolyte solution and application of bias bends the semiconductor bands such that, upon irradiation, electronic holes are driven to the surface. The electron-deficient Si surface is attacked by the carboxylate nucleophile, breaking a Si-Si bond and generating a silicon-ester species. A Si radical is also produced which abstracts  $\text{H}^+$  from solution. The esterified Si atom is subsequently oxidized by trace  $\text{H}_2\text{O}$ .

Si-F on the surface, also implicating the involvement of radical-abstraction reactions.

The above spectroscopic results are accounted for by a mechanism in which illumination of the reverse-biased Si wafer removes electron density from surface Si atoms, inducing nucleophilic attack by carboxylate (Figure 7). A Si-Si bond is broken to produce a Si-OOCR species as well as a Si radical which then abstracts  $\text{H}^+$  from solution. Reaction of the Si surface radical may be aided by the presence of  $\text{R}^*$  at the electrode from the photo-Kolbe decomposition of  $\text{RCOO}^-$ .<sup>62,63</sup> Esterification of a surface Si atom renders it susceptible to further oxidation (from trace  $\text{H}_2\text{O}$ ), forming a  $(\text{SiO})_x\text{H}_{3-x}\text{Si-OOCR}$  species.

The observed surface reactivity reflects the trend in relative bond energies of molecular Si compounds; Si-Si bonds are broken in preference to Si-H or Si-O bonds:<sup>71</sup> Si-Si (340 kJ/mol) < Si-C (360 kJ/mol) < Si-H (393 kJ/mol) < Si-O (452 kJ/mol) < Si-F (565 kJ/mol).

(71) Greenwood, N. N.; Earnshaw, A. *Chemistry of the Elements*; Pergamon Press: Oxford, 1984, pp 389.

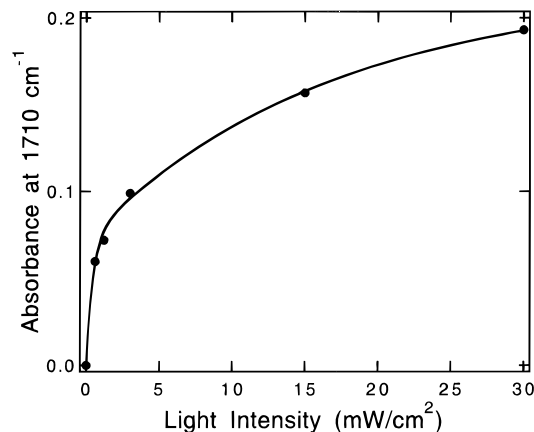
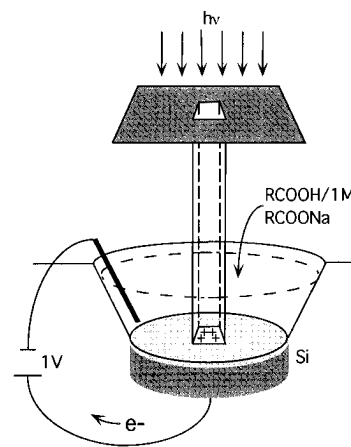


**Figure 8.** Intensity of the  $\nu(\text{C=O})$  absorption of the surface-bound ester as a function of the light intensity used in photoderivatization. The amount of ester increases with increasing light intensity. The points represent measurements made on six separate samples, after 5 min of irradiation at the indicated light intensities.

### Scheme 3



Previous studies of Si oxidation have shown that formation of the first Si-O bond is rate-limiting and is rapidly followed by O insertion into the remaining Si-Si bonds.<sup>56</sup> Oxidation of Si-H bonds is thermodynamically favorable but is so slow that it is generally not observed at room temperature.<sup>56,72</sup>

**Photopatterning Esters on Si.** The extent of esterification of the surface depends upon the light intensity used to drive photoelectrolysis (Figure 8). Under our experimental conditions (applied bias of +1 V, 1  $\Omega\cdot\text{cm}$  resistivity n-type Si), the rate of ester appearance is very sensitive to light intensity up to 3  $\text{mW}/\text{cm}^2$ . Above this level, the rate of reaction does not increase as dramatically with increasing light intensity, presumably because the rate becomes limited by mass transport in solution.

The sensitivity of the reaction to light intensity allows Si to be photopatterned with ester by illuminating the surface through a mask during derivatization (Scheme 3). Figure 9 shows a photograph of the photoluminescence from a circular porous Si sample with a square ester-modified region in the center. The ester-modified porous Si has a lower photoluminescence quantum yield presumably because the ester acts as an efficient non-radiative recombination center. Porous Si samples with surfaces containing a high concentration of ester are essentially non-emissive while samples with a lower concentration retain some photoluminescence intensity. Different locations on the ester-patterned Si surface in Figure 9 were sampled by diffuse

(72) Ito, T.; Yasumatsu, T.; Watabe, H.; Hiraki, A. *Jpn. J. Appl. Phys.* **1990**, 29, 201-204.

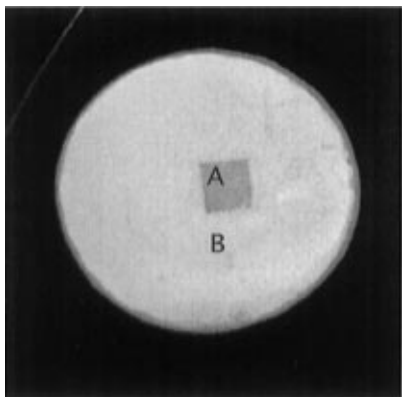


**Figure 9.** Photograph showing the photoluminescence of a circular 1-cm-diameter porous Si sample patterned with trifluoroacetic ester in a  $1.5 \times 1.5$  mm square region. The ester-patterned region is apparent as the less-luminescent square (labeled A) in the middle of the porous Si sample (labeled B). The photopatterned square was generated by illuminating the porous Si sample through a mask during derivatization, as illustrated in Scheme 3. The photograph was taken while exciting the porous Si with 365-nm light.

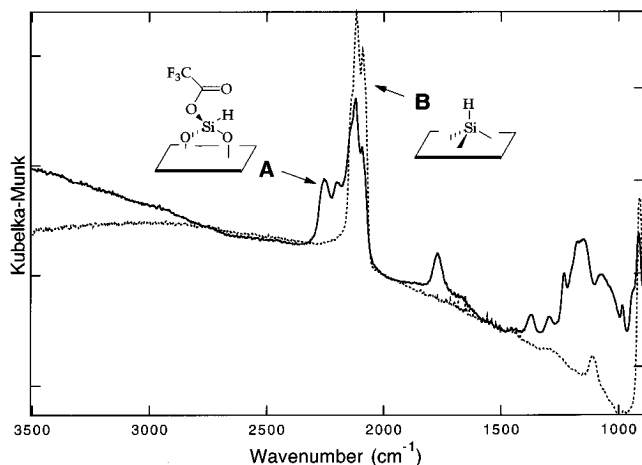


**Figure 10.** Diffuse reflectance FTIR spectrum of two regions of the sample shown in Figure 9. The solid line is a spectrum taken from the square region (labeled A in Figure 9) showing selective esterification of the surface. The dashed line is a spectrum of the region outside the photopatterned square (labeled B in Figure 9), which remains underivatized.

reflectance FTIR. The patterned square area contained the IR signature of surface-bound ester while the area outside the square displayed only the Si-H absorptions of the starting porous Si (Figure 10). Although we did not test the spatial resolution of the patterning technique, it is presumably limited by charge carrier mobility in the Si substrate.<sup>73</sup> The photopatterning technique should achieve higher resolution on porous Si samples relative to single-crystal Si, because photogenerated carriers are confined to nanocrystalline domains in porous Si.

The ester-modified regions of a photopatterned surface can be hydrolyzed to the simple oxide by exposure to acidic H<sub>2</sub>O. The simple oxide cannot be directly photopatterned onto the surface because H<sub>2</sub>O reacts with both the illuminated and non-illuminated regions of reverse-biased Si.<sup>65</sup>

**Chemical Reactivity of the Esterified Surface.** Esterification changes the chemical properties of the Si surface. In a preliminary report we have shown that the ester-modified surface is hydrophilic as opposed to the hydrophobic native hydride-terminated surface.<sup>11</sup> Reaction of a trifluoroacetic ester-modified surface with a 1% solution of organomethoxysilane,

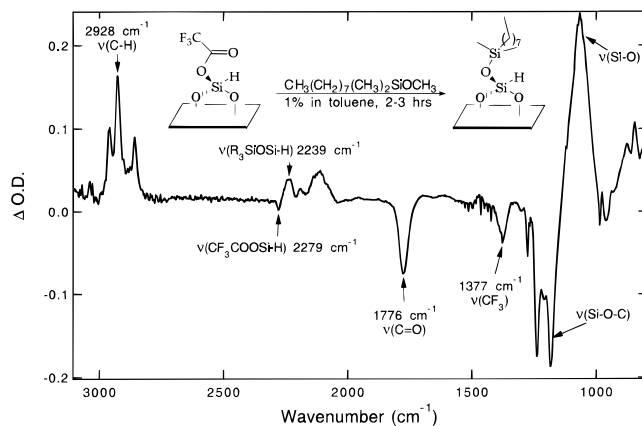


**Figure 11.** Difference infrared spectrum taken before and after reaction of the ester-modified porous Si surface with  $\text{CH}_3(\text{CH}_2)_7(\text{CH}_3)_2\text{SiOCH}_3$ . The spectrum shows the loss of surface-bound trifluoroacetate ester and appearance of organosilane.

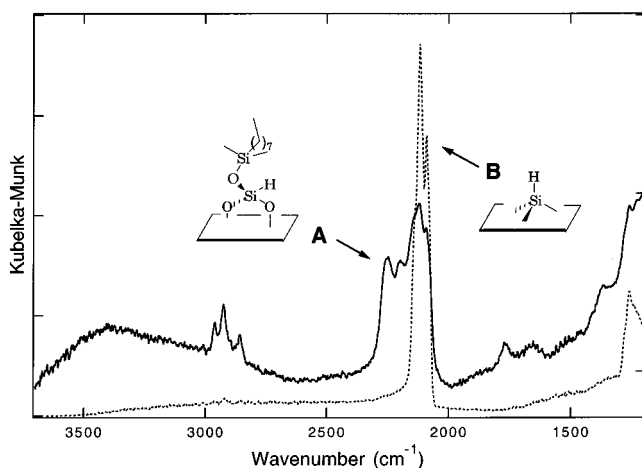


**Figure 12.** Diffuse reflectance infrared spectra of the patterned porous Si sample from Figures 9 and 10 following reaction with organomethoxysilane. The solid line is the spectrum taken from region A (the previously ester-modified region), showing attachment of organosilane. The dashed line is the spectrum from region B (the unmodified hydride-terminated surface), which shows no significant evidence of reaction.

$\text{CH}_3(\text{CH}_2)_7(\text{CH}_3)_2\text{SiOCH}_3$ , in toluene results in replacement of the ester with organosilane. A difference IR spectrum before and after reaction is marked by loss of the  $\nu(\text{C}=\text{O})$  vibrations from the trifluoroacetic ester and appearance of  $\nu(\text{C}-\text{H})$  stretches from the surface-bound  $\text{CH}_3(\text{CH}_2)_7(\text{CH}_3)_2\text{SiO}-$  group (Figure 11). The low-frequency side of the  $\nu(\text{OSi}-\text{H})$  band (assigned to  $\text{CH}_3(\text{CH}_2)_7(\text{CH}_3)_2\text{SiOSi}-\text{H}$ ) increases while the high-frequency side of the band (due to  $\text{CF}_3\text{COOSi}-\text{H}$ ) decreases in intensity. The absorption assigned to  $\nu(\text{Si}-\text{O}-\text{C})$  decreases and the lower frequency absorption assigned to  $\nu(\text{Si}-\text{O})$  increases. The replacement reaction probably occurs after *in situ* hydrolysis of the ester to the simple oxide by trace water.<sup>4</sup> The trifluoroacetic ester surface is found to be more reactive than the formic ester surface. The Si-H surface does not react with organomethoxysilane under these conditions.

Reaction of an organomethoxysilane and a Si-H surface patterned with an ester-modified region results in attachment of the organosilane exclusively on the esterified region. Figure 12 presents diffuse-reflectance infrared spectra of the ester-patterned porous Si sample from Figures 9 and 10 after it was allowed to sit in a solution of 1%  $\text{CH}_3(\text{CH}_2)_7(\text{CH}_3)_2\text{SiOCH}_3$  in toluene for 3 h. The spectrum of the patterned square region displays strong  $\nu(\text{C}-\text{H})$  absorptions at  $2928\text{ cm}^{-1}$ , assigned to

(73) Doan, V. V.; Sailor, M. J. *Appl. Phys. Lett.* **1992**, *60*, 619–620.

the organosilane, and only a small  $\nu(\text{C}=\text{O})$  vibration from residual ester. The native hydride-terminated Si surface outside the patterned region shows no evidence of reaction. The photoluminescence intensity from the photopatterned square is still very low after organosilanation, suggesting that this species is also a very efficient nonradiative recombination center. The unreacted region (outside the square) retains its photoluminescence intensity throughout the course of the derivatization experiments.

### Conclusions

We have presented a new photoelectrochemical reaction that generates a Si surface modified with formic, acetic, or trifluoroacetic ester species. The reaction involves photoinduced scission of Si-Si bonds and formation of a Si-ester species. Both porous and (100) single-crystal n-type Si undergo essentially the same chemistry. Due to the photochemical nature of this reaction, the ester products can be patterned on a surface lithographically.

The ester-modified and native hydride-terminated surfaces have significantly different properties, including hydrophilicity, chemical reactivity, and nonradiative surface recombination rate. We have demonstrated that organomethoxysilanes react specifically with the ester-modified and not the hydride-terminated regions of a patterned Si surface. The reactivity of Si esters provides a route to patterning Si surfaces with a variety of chemical reagents via the ester intermediate. This is the first reported general method for patterning Si with specific chemical functionalities by photoreaction with Si surface atoms.

**Acknowledgment.** This work was supported by the National Science Foundation (DMR-9220367) and a Camille Dreyfus Teacher-Scholar and Sloan Foundation fellowship (to M.J.S.). T.W.B. and J.S.H. were supported by NSF Research Experiences for Undergraduates Fellowships.

JA960777L